In Situ Nanomechanical Characterization Techniques for Soft Bioelectronic Interfaces and Their Building Blocks

Giorgio Cortelli, Tobias Cramer,* Luca Patruno, Beatrice Fraboni, and Stefano de Miranda

Soft bioelectronic interfaces constitute a paradigm shift for biomedical devices. High-resolution monitoring and stimulation of physiological processes in vivo are becoming possible with minimally invasive devices operated without inflicting tissue damage or discomfort over prolonged timescales. However, the development and commercialization of such interfaces still must address significant challenges. Biological tissue is subjected to continuous motion and the related device deformations can easily trigger fracture or delamination of the device components, putting long-term durability of soft implants at risk. In this review, an overview of experimental techniques for testing mechanical properties and failure mechanisms of soft bioelectronic devices at the nanoscale while the deformation takes place (in situ) is provided. Through the tensile test, bending test, nanoindentation, and micropillar compression test, precise measurements of the mechanical properties of individual building blocks and the interfaces themselves can be obtained. Such parameters are crucial to design, model, and optimize the device's performance. Then, recent examples of how this information guides design and optimization of soft bioelectronic interfaces and devices for healthcare, robotics, and human–machine interfaces is provided. Last of all, future research that is needed to fully achieve long-term soft bioelectronic interfaces for integration with the human body is discussed.

1. Introduction

Bioelectronics is based on the transduction of signals between tissue and device interfaces, enabling the measurement and control of biological processes for diagnostic and therapeutic uses in healthcare applications.[1,2] Bioelectronic interfaces have significant potential for both therapy and diagnosis as they can measure physical, electrical, and chemical signals in the body.[3–7] Physical biosensors can detect physical signals, such as body motion,[8,9] heart rate, and blood pressure;[10–13] while, electrophysiological signals can be captured via electrocardiography , electromyography , and electroencephalography . Nevertheless, the most crucial element of implantable devices is centered around the recording and modulation of neural signals. This is accomplished by directly interfacing with neural tissue using invasive electrodes. This bidirectional communication can monitor and stimulate the central[14] or peripheral[15] nervous system, making it crucial for the diagnosis and therapy of neural diseases. Moreover, the real-time monitoring of biochemical markers, including pH, ions, glucose, and lactate, offers comprehensive insights into an individual's health, performance, or stress on a molecular level.[7,16]

This underscores the immense potential of utilizing bioelectronic interfaces to enhance patient outcomes across a broad spectrum of medical disciplines.

As the human body is inherently soft and in continuous mechanical motion, bioelectronic interfaces have to comply with movements of the human body to be biocompatible, stable, and safe during long-term operation.[17–21] Understanding the mechanical response of wearable and implantable devices during deformation is crucial for optimizing their performance, improving their biocompatibility, and increasing their lifespan. Conventional stiff bioelectronic interfaces cannot conform to soft and curvilinear skin or tissue or adapt to body motions, leading to performance issues and high impedance.[22,23] Friction between stiff wearable devices and skin can cause rashes, inflammation, and even allergic reactions.[24,25] In the body, stiff implanted bioelectronics can trigger foreign body responses and inflammatory reactions that lead to scar tissue formation, causing increased electrical impedance and reduced recording performance.[26–28] Increased electrode impedances cause further degradation due to water electrolysis and radical formation happening at increased electrode potentials. Instead, degraded isolation materials cause

G. Cortelli, L. Patruno, S. de Miranda
Department of Civil, Chemical, Environmental, and Materials Engineering
University of Bologna
Viale del Risorgimento 2, Bologna 40136, Italy
T. Cramer, B. Fraboni
Department of Physics and Astronomy
University of Bologna
Viale Berti Pichat 6/2, Bologna 40127, Italy
E-mail: tobias.cramer@unibo.it

**ADVANCED
SCIENCE NEWS**

www.advancedsciencenews.com

**ADVANCED
MATERIALS
TECHNOLOGIES**

www.advmattechnol.de
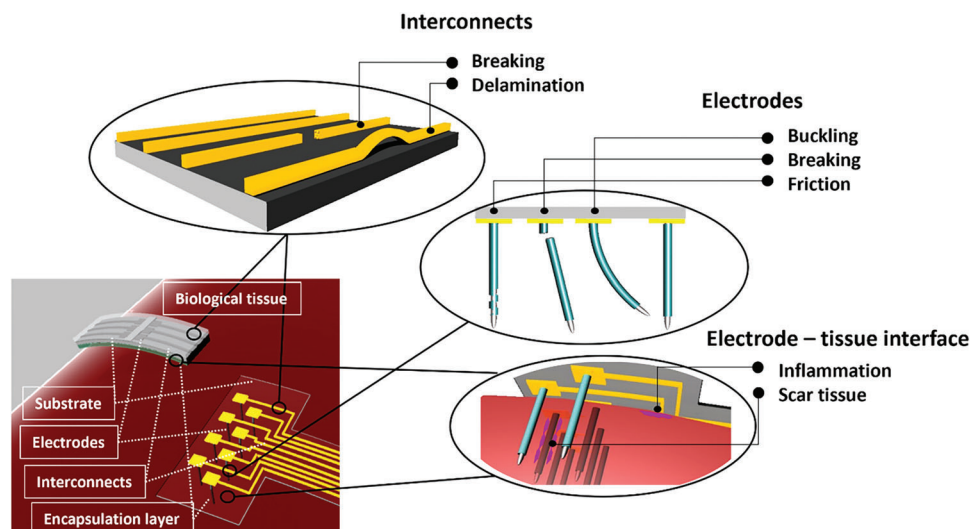
Figure 1. Soft bioelectronic interface. On the bottom left, a schematic of a wearable (left) and implantable (right) soft bioelectronic interface in contact with biological tissue is shown. The image shows the main components of a soft bioelectronic device: substrate, electrodes, interconnects, and encapsulation layer. The encapsulation layer is shown in light blue. It covers the interconnects and parts of electrodes that should not exchange signal with biological tissue. The inset on the top left shows typical failure modes (breaking and delamination) that can occur in the interconnects under device operating condition. The inset in the center presents different failure mechanisms of 3D electrodes (buckling, breaking, and friction of the encapsulation layer). For the case of 2D electrodes, they can be damaged by friction as well as by breaking or delamination. The bottom right inset shows the main interfaces between the device and the tissue. In the case of wearable and the non-inserted part of the implantable device, inflammation can occur due to the mechanical mismatch. For implantable devices, the foreign body response can cause scar tissue formation, leading to an increase in impedance.

increased leakage currents and unwanted electrochemical reactions.[29]

In recent years, significant advances in flexible and stretchable electronics have been obtained leading to soft bioelectronic interfaces.[30–35] Soft bioelectronic devices need to be designed for long-term use and must adapt to mechanical strains; while, maintaining good tissue coupling.[36–40] Soft bioelectronic interfaces aim to avoid the mechanical mismatch by using materials that are soft and flexible, allowing the devices to conform to the shape of biological tissues without causing damage or discomfort. To address these issues, new materials and manufacturing techniques have been developed that can produce devices with mechanical properties more closely matched to biological tissues.[41–47] This includes the use of materials such as hydrogels and polymers, which are soft and biocompatible and implement dynamic stress relaxation, toughness, and self-healing properties.[42] Dynamic stress relaxation allows stretchable materials to endure repeated stretching and recover their original shape without permanent damage. Toughness ensures that stretchable materials can handle substantial strain or deformation without breaking. Self-healing characteristics enable stretchable materials with dynamically crosslinked bonds to repair or re-establish their bonds when damaged during stretching or deformation. The combination of these properties makes stretchable materials with dynamically crosslinked bonds highly desirable for applications such as flexible electronics, wearable devices, and biomedical implants, where mechanical durability and self-repair capabilities are crucial for long-term performance and reliability.[48,49]

Manufacturing strategies to develop devices that can stretch and deform without causing damage to the tissue or the device are based on several components usually made of materials with different mechanical properties. Typically, the building blocks of soft bioelectronic interfaces can be classified into four categories: 1) the substrate, 2) the interconnects, 3) the electrode, and 4) the encapsulation layer.[50] The substrate serves as the physical support for the device and can be made of various materials such as polymers, ceramics, or metals. The layer with interconnects is the active layer of the device and can include materials such as conductive polymers, hydrogels, or nanowires. The electrode is the component that interfaces with the biological tissue and can be made of conductive metals such as gold or platinum, and also of conductive hydrogels, conductive polymers, or conductive fibers. Finally, the encapsulation layer is responsible for protecting the device from the surrounding environment and can be composed of polymers or other biocompatible materials.[51] A schematic of soft bioelectronic devices interfacing with a biological tissue is shown at the bottom of **Figure 1**.

Despite the improvements from rigid to soft bioelectronics, achieving a good match between the mechanical properties of the device and the tissue is still a major challenge, especially when considering long-term implantation and use of the devices. Surface morphology of both the device and the heterogeneous body parts plays a crucial role in determining the performance of bioelectronic soft interfaces and their failure modes as the surface is the point of contact between the sensor and the body.[50] As for rigid bioelectronic interfaces, it is crucial to avoid the mechanical mismatch due to stiffness incompatibility among different layers of the soft device and between the device itself and the biological tissue. In addition, developing flexible and stretchable soft devices based on multiple layers and building blocks with different material properties introduces new critical mechanical issues. Delamination of the functional layer from the substrate, for example, typically can occur as a result of compression or bending of the soft device.[52–54] The formation of microcracks large

enough to render the electrode or interconnects nonconductive can be caused by excessive stretching or bending of a single device component.[55–57] In addition, it is not guaranteed that soft bioelectronic interfaces can withstand mechanical loads during handling and insertion. In fact, the device must reach its operating target location without triggering mechanical failure modes such as buckling, cracking, delamination, or excessive friction between the encapsulation layer and the biological tissue.[52,58–60] An illustration of the main mechanical failure modes of the different components of a soft bioelectronic device is reported in Figure 1.

Microscopic mechanical characterization is mandatory to understand the activation of failure mechanisms and optimize the devices coupling with the biological tissue; for example, to detect fracture of interconnects or partial damage to a microelectrode. However, microscopic characterization alone is not sufficient to provide all the information needed in the investigation and optimization of mechanical properties of soft bioelectronic devices. Indeed, the failure mechanisms mentioned above occur while the device is operating under strain in different configurations, such as stretching or bending, as well as compression. Therefore, mechanical characterization techniques, performed during the deformation, are needed to reveal insights into the nanoscale mechanisms causing device failure. Throughout this manuscript, we refer to the term in situ as those characterization techniques that take place during deformation. Conducting in situ, localized micromechanical tests on individual components, along with assessing their inherent properties, presents practical obstacles. These challenges include the need to examine samples at the nanoscale, precisely manipulate the sample for mechanical testing, and accurately measure the applied force and deformation during the process. Traditional universal material testing machines are generally suited for testing objects manageable by hand and don't demand direct observations at the microscale.[61] The most used instruments for soft bioelectronics mechanical characterization are the universal testing machine (UTM) and dynamic mechanical analyzer (DMA). UTM is versatile and commonly used for materials testing and characterization, allowing to perform tensile, compression, bending, and shear tests on soft materials.[45,47] DMA evaluates viscoelastic properties, crucial for understanding time-dependent mechanical behavior in soft bioelectronic interfaces.[48,49] These instruments enable the assessment of overall device performance under operating conditions. Unfortunately, the relatively small size of the individual component cannot be observed without the aid of a microscope. In addition, a greater manipulation precision and force resolution than provided by conventional methodologies is required. It therefore turns out to be necessary to complement standard global tests of the whole device with local in situ tests to have a greater understanding of deformation phenomena. Therefore, a rational optimization process of soft bioelectronic devices can only occur when mechanical testing is combined with specific experimental setups for local in situ characterization supported by predictive models. Only a deeper understanding of these mechanical aspects will pave the way to an optimized design of wearable and implantable soft bioelectronics initiating a new era of health monitoring, diagnosis, and therapeutics.

In this work, we review in situ nanomechanical characterization methods to study soft bioelectronic interfaces and their building blocks, such as nanowires, nanofibers, nanopillars, and ultra-thin films. Reported techniques for in situ local nanomechanical testing used various microscale imaging techniques such as atomic force microscopy (AFM), confocal laser scanning microscopy (CLSM), scanning electron microscopy (SEM), and transmission electron microscopy (TEM). The instrument to perform the mechanical test was placed inside the chamber of the imaging tool to observe the samples during the acquisitions. Recently, specific instruments, such as microelectromechanical systems (MEMS) or AFM cantilevers to achieve controlled microscale deformations have also been adopted. In advancing our understanding of soft bioelectronic interfaces, in situ nanomechanical characterization techniques play a crucial role by providing valuable insights into their mechanical behavior under real operating conditions. These methods enable researchers to investigate the intricate mechanics of these interfaces at nanoscale resolutions, shedding light on the underlying processes and interactions that govern their functionality. However, it is important to acknowledge the limitations associated with these techniques. Notably, the size constraints of soft bioelectronic devices can be challenging as some nanomechanical testing methods require minimum sample sizes for accurate measurements. Manipulating and positioning very small or thin devices may affect the accuracy of the results. In addition, the delicate nature of soft bioelectronic samples requires careful preparation for nanomechanical testing. The handling and mounting process may inadvertently alter the mechanical properties of the samples and introduce artifacts, potentially impacting the experimental outcomes. Moreover, maintaining physiological conditions during nanomechanical testing poses challenges. Variations in temperature, humidity, or pH levels can influence the mechanical behavior of the samples, leading to discrepancies between in situ measurements and real-world performance. Despite these limitations, the significance of in situ nanomechanical characterization techniques cannot be overstated. They remain indispensable tools in bioelectronic interface research, offering unique insights into the mechanical properties and behavior of soft interfaces under realistic conditions. Understanding these mechanical responses helps optimize the design of more robust, reliable, and biocompatible bioelectronic devices. It is essential to consider in situ nanomechanical techniques as complementary rather than substitutive to other global characterization methods such as UMT or DMA. By integrating diverse approaches, researchers can gain a comprehensive understanding of soft bioelectronic interfaces, bridging the gap between macroscopic and nanoscale behavior, and driving groundbreaking advancements in bioelectronics.

To structure the review, we first consider the main modes of deformation to which a soft bioelectronic interface is subjected both during insertion and during its long-term operation. As previously mentioned, devices are mainly subjected to stretching, bending, and compression. Accordingly, this work is organized into three main sections related to what deformation mode is activated during the in situ nanomechanical characterization tests: tensile, bending, nanoindentation, and micropillar compression. The final, most relevant section is dedicated to case studies in which such nanomechanical characterization techniques have been employed to enhance the mechanical performance of soft

**ADVANCED
SCIENCE NEWS**

www.advancedsciencenews.com

**ADVANCED
MATERIALS
TECHNOLOGIES**

www.advmattechnol.de

Table 1. Summary of the discussed in situ nanomechanical tensile tests. The table shows the properties that can be measured and the kind of sample that can be investigated with the proposed technique as described in the referenced articles.

Measurements	Samples	References
	Tensile test	
Elastic modulus	Nanowires and thin films	Zhu et al.[62]
	Thin films	Cao et al.[63]
	Thin films	Costa Angeli et al.[64]
Delamination	Thin films	Costa Angeli et al.[65]
Tensile strength	Nanofibers	Hang et al.[61]
Yield strength	Thin films	Thomas et al.[66]
Stiffness and conductivity	Thin films	Cortelli et al.[67]
Fatigue	Thin films	Cattarinuzzi et al.[68]

bioelectronic interfaces. In the conclusions, we discuss the challenges that need to be addressed before soft bioelectronic interfaces can achieve long-term integration with the human body.

2. Tensile Test

The traditional tensile test conducted at the macroscale consists in subjecting a specimen, typically of dog-bone shape, to a uniaxial increasing load resulting eventually in the sample failure. The tensile test can be used to determine several characteristics of the material under test, including Young's modulus, yield strength, and ultimate strength. In recent years, tensile tests have been trying to reproduce at the nanoscale with different experimental setups. In the context of soft bioelectronic interfaces, such an approach is crucial to investigate how is the response of the device and its building blocks under stretching.[7] The added value of developing techniques for in situ tensile testing lies in the ability to observe the onset and evolution of damage of single components and their assembly as the load is applied. In **Table 1** is summarized the in situ tensile test discussed below.
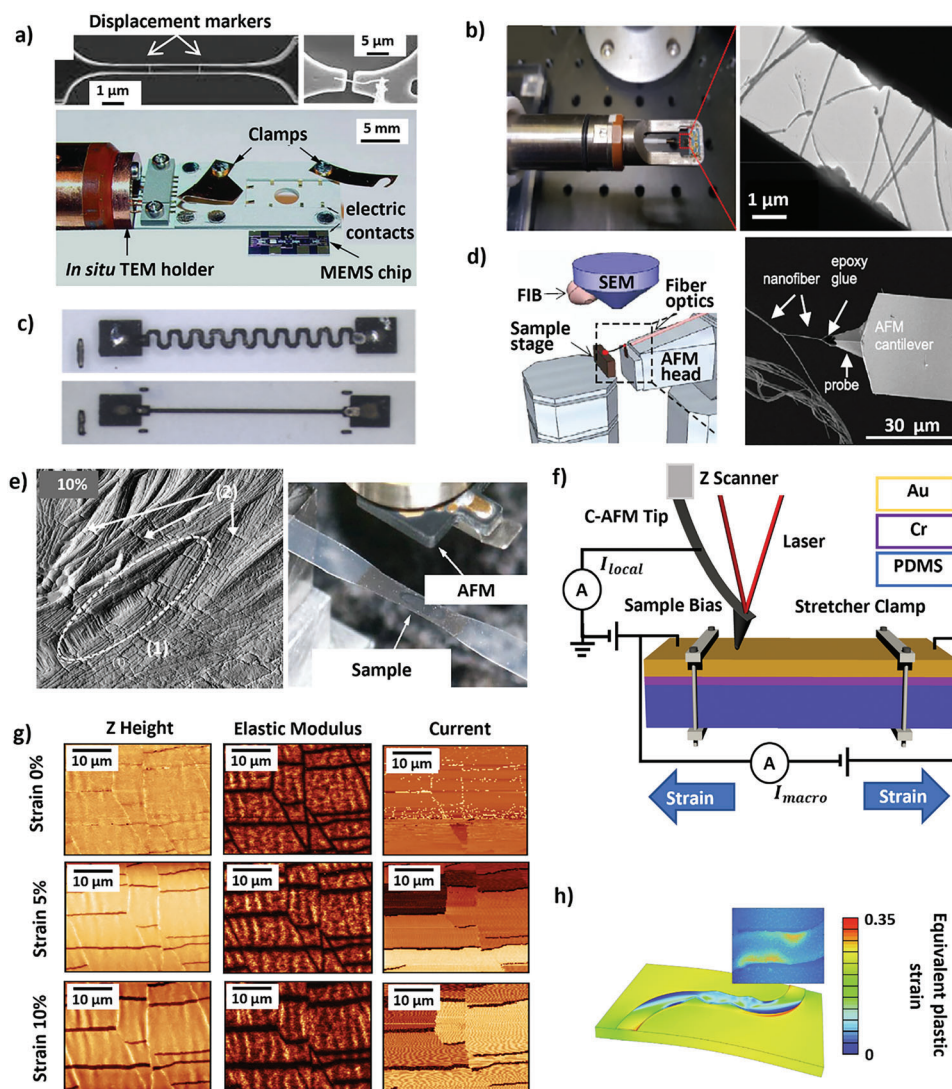
The elastic modulus is a key parameter to estimate for soft bioelectronic devices as it has a direct impact on the mechanical mismatch with biological tissue. The ability to estimate this parameter for each device component provides a method to also understand the interaction and mechanical mismatch between the various building blocks. In this context, Zhu et al.[62] devised a material testing setup to enable in situ electron microscopy and mechanical testing of nanostructures. This testing configuration incorporates a microelectromechanical system (MEMS) containing an actuator (electromechanical or thermomechanical) and a load sensor based on capacitance measurement. To observe the specimen during the uniaxial tensile test, they used either a SEM or a TEM and monitored two displacement markers during the acquisition (**Figure 2**a). To test their experimental setup, they investigated different free-standing nanostructures, such as carbon nanotubes, palladium nanowires, and polysilicon films, acquiring the stress–strain curves. In the case where nanofibers were embedded in a polymer matrix, Cao et al.[63] proposed in situ tensile testing by exploiting the ability of TEM to obtain surface information of the sample but not just that. Specifically, they considered graphene hybrid films with Ag nanowires. The sample and

the experimental setup can be seen in Figure 2b. Their findings highlight a softening of the hybrid films compared to a single graphene film. Similarly, Costa Angeli et al.[64] performed tensile tests to investigate the strain sensing behavior of 3D printed carbon nanotubes percolation matrix. The resistive strain sensor array, produced using all-inkjet printing, successfully mapped the deformation of the substrate surface. The initial step involved examining the strain-sensing characteristics of the printed CNTs percolation network by creating and electromechanically assessing a single sensor. Further, a confined electromechanical tensile test was conducted on the manufactured sensor array, applying a non-uniform strain distribution. The outcomes demonstrated that the deformable sensor array, printed using inkjet technology, possessed the capacity to depict distinct local strains across the substrate surface.

The in situ tensile test can also be a valid method for investigating delamination between layers of the same device. For example, with the same micro-tensile tester and a confocal laser microscope, Costa Angeli et al.[65] developed and studied inkjet printed interconnects using both linear and serpentine shapes on two distinct substrates (Figure 2c). The findings revealed that the printing quality and the electromechanical response were significantly influenced by the geometrical layout and printing direction. An AFM was employed by Hang et al.[61] as mechanical tester in studying the mechanical properties of nanofibers. The evaluation of individual nanofibers' mechanical properties took place within the SEM chamber, which was equipped with an AFM system. To facilitate this, a specially designed AFM setup was employed, where the sample stage was oriented at a 90° angle to a typical AFM configuration. This adjustment enabled exposure to the SEM's electron beam. Precise manipulation was achieved by maneuvering the AFM probe, affixed to a cantilever, using a piezo scanner linked to the AFM head. The nanofiber under investigation was glued on both sides, one to a substrate and one to the AFM tip. A scheme of the experimental setup as well as a glued nanofiber to the AFM tip before the acquisition are shown in Figure 2d. The nanofibers were tested by applying a uniaxial tensile load moving the AFM tip. Force spectroscopy showed increased tensile strength and elastic modulus when compared to bulk equivalents. Measurements of this kind are crucial for the development of optimized soft bioelectronic interfaces as they allow tuning of the mechanical properties of the device, based on its target.

As devices whose goal is to remain implanted or worn for a long time, it is necessary for the performance of the device to be stable over time. Therefore, it is important to estimate the yield strength of the components and of the entire device to characterize the onset of the plastic response of the material. Once this threshold value is exceeded, in fact, the device will undergo permanent deformation. Thomas et al.[66] developed an experimental configuration aimed at studying the plastic deformation mechanism of semi-crystalline polymers. This setup involves capturing images from the same point on the sample as strain is applied, allowing for the observation of changes over the deformation process. The strain is applied and monitored with a motorized stretching stage which is placed under the AFM probe to capture images of the sample while stretching. In particular, they studied the initiation, growth, and coalescence of crazes in poly(1-butene) at different strain values. Figure 2e shows an image of

**ADVANCED
SCIENCE NEWS**

www.advancedsciencenews.com

**ADVANCED
MATERIALS
TECHNOLOGIES**

www.advmattechnol.de

Figure 2. Tensile test. a) The setup features an in situ TEM holder paired with a 5 × 10 mm MEMS chip. In the experimental configuration, the MEMS chip is flipped and positioned within the TEM holder; then, firmly secured using the left and right clamps. The two SEM images on top show the working configuration of both a thin film and a nanowire. Adapted with permission.[62] Copyright 2005, National Academy of Sciences. b) In situ TEM tensile testing platform of Ag NW/graphene hybrid film sample. Reproduced under the terms of the CC BY 4.0 license.[63] Copyright 2020, The Authors, published by International Journal of Smart and Nano Materials. c) Linear and serpentine inkjet-printed interconnects. Reproduced with permission.[65] Copyright 2019, Springer Nature. d) AFM-in-SEM configuration for in situ nanofiber tensile test. The image on the right shows the glued nanofiber attached to the AFM probe before the acquisition. Adapted with permission.[61] Copyright 2011, IOP Publishing. e) On the left, the AFM image of the diagonal region of spherulite at 10% strain is shown. The label (1) denotes the initiation of crazes at the interface between lamella stacks displaying distinct orientations; while, label (2) indicates the fragmentation of lamellae within a single lamella stack. Reproduced with permission.[66] Copyright 2007, Elsevier. f) AFM setup for in situ multichannel mapping of metallic thin films on polymers. Reproduced under the terms of the CC BY 4.0 license.[67] Copyright 2022, The Authors, published by American Chemical Society. g) Microcracks evolution as a function of tensile strain. The figure shows the three-channels maps: morphology, elastic modulus, and current at different strain values (0%, 5%, and 10%). Reproduced under the terms of the CC BY 4.0 license.[67] Copyright 2022, The Authors, published by American Chemical Society. h) FEM outcomes are presented alongside the mixed-mode cohesive zone model. For comparison, the insets display topographic height profile measurements obtained from experiments conducted at the corresponding global stretch increment. Reproduced under the terms of the CC BY 4.0 license.[69] Copyright 2020, The Authors, published by Elsevier.

the samples obtained using SEM with 10% strain. Their findings show the presence of crazes oblique to the principal tensile stress. In addition, the tensile test allowed to investigate the formation and growth of microcracks till they reached a width large enough to cause a significant drop in electrical conductivity of the device. For example, Cortelli et al.[67] designed an experimental setup

combining an AFM and a strain stage to investigate in situ, the mechanically induced electrical properties of thin metal films on a polymeric substrate under tensile strain (Figure 2f). In particular, the AFM was exploited for a three-channels acquisition: morphology, stiffness, and conductivity. The approach utilizes rapid and repetitive nanoindentation experiments (force spectroscopy)

in conjunction with a conducting AFM probe. These experiments are conducted on a freestanding stretched sample, enabling the acquisition of multichannel images at varying strain levels. In order to validate the experimental configuration, the researchers analyzed the propagation of microcracks in a thin gold film deposited on polydimethylsiloxane (PDMS). This technique permitted the observation of microcrack formation during tensile strain and its impact on local current conduction and surface mechanics. Figure 2g presents the morphology, elastic modulus, and conductivity maps of the same sample area under different strain conditions. The results indicate that, even as the film fractures into distinct fragments, higher strains sustain current conduction through a tunneling mechanism.

So far, tensile test experiments that reach the sample failure within a single acquisition have been reported. Nevertheless, it is also crucial to investigate the material behavior at the nanoscale under cyclic load, that is, under multiple usages. This is the case of the fatigue test, which consists of the application of a cyclic load to the sample, keeping the maximum load in the elastic regime. These tests serve the purpose of generating data related to fatigue life and crack growth, pinpointing critical locations, or validating the structural integrity of components that could be vulnerable to fatigue. For example, Cattarinuzzi et al.[68] investigated the failure mechanism of aluminum/polyimide stretchable interconnects under cyclic load with a uniaxial stress test with in situ SEM or CLSM. Their work highlights the crucial role played by the interface between the substrate and the metal serpentine in defining the mechanical properties of the stretchable interconnects. During the process of stretching the substrate, the stress that affects the interconnect metal core is alleviated by the deformation of the winding structure. This structure undergoes both in-plane and out-of-plane distortions. Further, the compliant substrate beneath provides additional support, contributing to a delay in the occurrence of ductile failure in the metal film. In a subsequent work, Kleinendorst et al.[69] used the same experimental setup with CLSM to extract height profiles of metal serpentines on polyimide. Using a digital height correlation algorithm, they recorded the 3D microscopic deformation both in-plane and out-of-plane. They then compared the experimental results with numerical simulations to model and describe the behavior of the interface during the experiment. The comparison between experiments and simulations suggests that only considering residual stresses and different properties in shear and normal directions allows a comprehensive description of the delamination mechanism. A simulation result and a CLSM image are compared in Figure 2h.
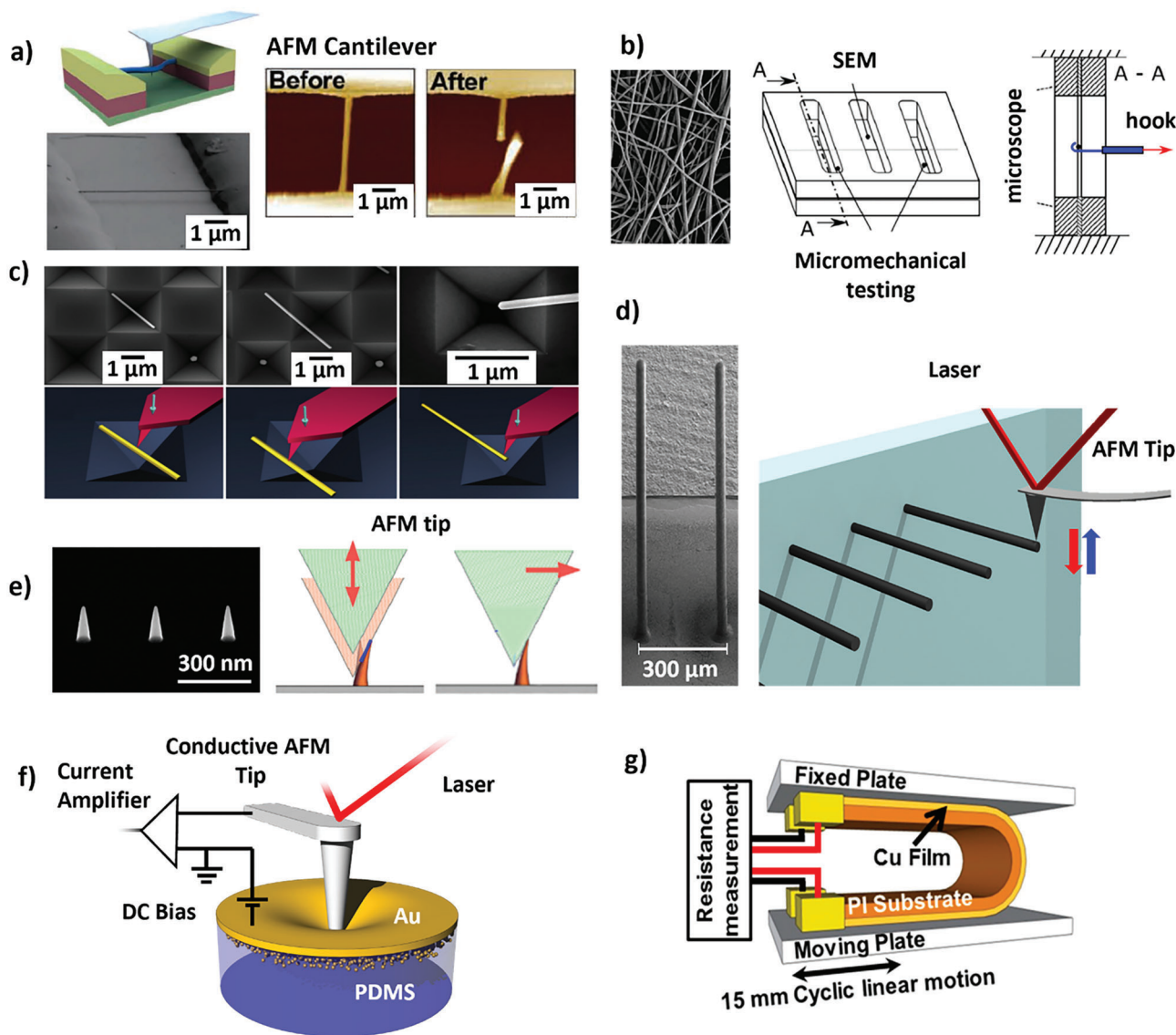
3. Bending Test

In a macroscopic bending test, specimens are typically characterized by a geometry for which one (two) dimension(s) are greater than the other two (one) and can be modelled as beams (plates). These specimens are loaded perpendicularly to the longitudinal axis (middle plane) identified from the sample geometry. Depending on the geometry of the specimen, different experimental setups are used and allow for the investigation of its mechanical properties, such as the bending stiffness, the maximum deflection, and the failure stress. Typical soft bioelectronics building blocks tested under bending are nanowires, nanofibers, nanopil-

Table 2. Summary of the discussed in situ nanomechanical bending tests. The table shows the properties that can be measured and the kind of sample that can be investigated with the proposed technique as described in the referenced articles.

Bending test		
Measurements	Samples	References
Ultimate strength	Nanowires	Kim et al.[70]
Elastic modulus	Nanofibers	Morel et al.[71]
Elastic modulus	Nanowires	Antsov et al.[72]
Bending stiffness	Micropillars	Cortelli et al.[73]
Bending stiffness and failure stress	Nanopillars	Angeloni et al.[74]
Bending stiffness	Thin films	Abrahamians et al.[75]
Elastic modulus	Thin films	Cortelli et al.[76]
Fatigue	Thin films	Kim et al.[78]

lars, or thin films. **Table 2** reports a summary of the in situ bending tests and the characterized micromechanical properties described below.

Structures such as nanowires and nanofibers are often used in soft bioelectronic devices, especially in the functional layer. Therefore, the electrical conduction of the device depends on them. Such components can be exploited as functional layers in soft bioelectronic devices either embedded in a polymer matrix or deposited on a softer substrate. Quantitative estimation of bending stiffness, which is elastic modulus dependent, allows the mechanical mismatch between the device and the target tissue to be evaluated. The added value of applying in situ characterization is that one can observe the component or device during testing. This makes it possible not only to evaluate maximum deflection and failure stress but also to understand at what point the failure mechanism is activated. Due to the small size of the samples, a microscope is crucial to observe the sample and apply the load at the desired location and direction. In addition, the ability to investigate the mechanical response of the single component (nanowire) at the nanoscale provides fundamental information for tuning the mechanical properties of the device. For example, Kim et al.[70] explored the nanomechanical characteristics of silicon nanowires with radii ranging from 15 to 70 nm using AFM bending on freestanding samples. In this case, the nanowires were clamped on both ends, as shown in **Figure 3**a. In particular, results highlight that under a minimum threshold radius, the mechanical properties show significant size dependency because the nanowire strength dramatically increases as the radius is reduced. Similarly, Morel et al.[71] investigated the micromechanical properties of poly(L-lactide) nanofibers of different diameters with AFM bending. To apply the load at the center of the nanofiber, a hook was used. The experimental setup and the sample during the acquisition can be found in Figure 3b. Young's moduli show a strong increase for thinner fibers below a critical diameter of 800 nm. Antsov et al.[72] used AFM to measure the elastic modulus of fivefold twinned gold nanowires and compare three different sample configurations to perform the acquisitions. Specifically, they tested the following configurations: three-point bending with fixed ends, three points bending with free ends, and cantilevered-beam bending. The configurations

**ADVANCED
SCIENCE NEWS**

www.advancedsciencenews.com

**ADVANCED
MATERIALS
TECHNOLOGIES**

www.advmattechnol.de

Figure 3. Bending test. a) SEM images of fabricated structures and AFM bending configuration. AFM images before and after the bending are reported on the right. Adapted with permission.[70] Copyright 2010, Wiley-VCH GmbH. b) On the left, the electrospun nanofibers are shown. On the right, the micromechanical testing setup is reported. The hook used to apply the load to the fibers is drawn in blue. Adapted under the terms of the CC-BY-NC-ND license.[71] Copyright 2018, The Authors, published by Elsevier. c) SEM images, accompanied by corresponding schematics, showcasing Au NWs in three different configurations: free-ends (left), fixed-ends (center), and cantilevered (right). Reproduced with permission.[72] Copyright 2019, Elsevier. d) SEM image of PA 3D inkjet printed with a thin metallic coating and a schematic of the AFM experimental setup to investigate their bending. Reproduced under the terms of the CC-BY 4.0 license.[73] Copyright 2023, The Authors, published by American Chemical Society. e) SEM image of the nanopillars under investigation. On the right, the force spectroscopy imaging approach and the contact mode imaging method are shown, respectively. Adapted under the terms of the CC-BY 4.0 license.[74] Copyright 2021, The Authors, published by Elsevier. f) Scheme of the AFM experimental setup for nanomechanical and electrical characterization of thin metallic layers on elastomeric substrate. Reproduced under the terms of the CC-BY 4.0 license.[76] Copyright 2021, The Authors, published by American Chemical Society. g) Schematic of the bending fatigue test and an electrical resistance monitoring system. Reproduced under the terms of the CC-BY 4.0 license.[78] Copyright 2019, The Authors, published by MDPI.

are depicted in Figure 3c. In addition, all three setups were subjected to finite element simulations to provide enhanced comprehension of the stress distribution within nanowires during bending, as influenced by the specific testing conditions.

Nanopillars are the components that interface with the biological tissue to be monitored or stimulated. They are composed of a conductive material and an encapsulation layer that isolate the

conductive part except where required. Bending test is crucial for these structures as it gives insight into whether the electrode will be able to be inserted correctly in contact with the tissue or whether it will undergo buckling or breaking. This type of characterization is crucial because while in order to avoid damage to the 3D electrode (pillar), the ideal would be to develop it as rigidly as possible, excessive stiffness leads to activation of the foreign body

2300931 (7 of 16)

**ADVANCED
SCIENCE NEWS**

www.advancedsciencenews.com

**ADVANCED
MATERIALS
TECHNOLOGIES**

www.advmattechnol.de

response; and thus, to an increase in electrical impedance, preventing the soft bioelectronic interface from functioning. In this contest, the possibility of in situ nanomechanical characterization allows monitoring not only the pillar breakpoint but also the state of the encapsulation layer. In fact, this layer of material tends to be thinner than the conductive part of the pillar and made of an extremely softer material. Therefore, the impact on the mechanical response of the device alone is negligible. However, delamination or damage of the encapsulation layer dramatically decreases the performance of the device. Cortelli et al.[73] showcased an experimental approach solely relying on AFM force spectroscopy, which furnished measurements for both the stiffness of a micropillar and the elastic modulus of its constituent material. This methodology was validated using four distinct varieties of 3D inkjet-printed micropillars: silver micropillars sintered at temperatures of 100 °C and 150 °C and polyacrylate microstructures with and without a metallic coating. The obtained elastic moduli were observed to be comparable with the corresponding bulk values. Moreover, their findings indicate that neither the sintering temperature nor the presence of a thin metal coating significantly influences the mechanical characteristics of the micropillar. A SEM image of the micropillars and a schematic of the experimental setup are shown in Figure 3d. An experimental approach to characterize micromechanical properties of nanopillar in vertical rather than freestanding configuration has been recently proposed by Angeloni et al.[74] They introduced two atomic force microscopy-based techniques: contact mode imaging and force spectroscopy imaging. These methods enable the assessment of mechanical properties of individual micro- and nanopillars in their as-fabricated state, without using SEM. Figure 3e shows the samples as well as the working principle of both techniques. The technique has been tested either on polymeric nanopillars or electron beam-induced deposited nanopillars. With the proposed technique, authors were able to estimate the stiffness of the nanopillars, as well as the maximum lateral force, the maximum deflection, and the failure stress.

Bending test performed on thin films provides direct access to evaluate the stiffness of the conductive layer of the bioelectronic device. In situ mechanical characterization makes it possible to directly observe the formation and evolution of micro- and nanocracks that, when too wide, render the functional layer nonconductive; and thus, the device unusable. However, the formation of microcracks is one of the techniques for obtaining a conductive and stretchable material. In situ nanomechanical characterization; therefore, allows the study of the flexural limit beyond which the device can no longer be used and also to test different crack arrangements to optimize this threshold value according to the application. These types of measurements are critical in predicting whether the device will be able to operate properly and evaluate the level of mechanical mismatch between the device and the tissue. In this context, Abrahamians et al.[75] developed an experimental setup to perform in situ stiffness measurements on ultrathin membranes. More precisely, the local stiffness of suspended indium phosphite (InP) membranes was gauged by making contact at various locations on their surface. This was achieved using a self-sensing quartz tuning fork probe regulated under frequency modulation. These tests were carried out in a controlled manner within a SEM, utilizing the in situ capabilities of a robotic nanomanipulation system. Cortelli et al.[76] investi-

gated the bending of thin metal films on polymeric substrates employing AFM force spectroscopy. The resulting method enabled quantification of the local Young's modulus of elasticity of the nanometer-thick film. A schematic of the experimental setup is reported in Figure 3f. The technique has been tested investigating gold thin films on PDMS substrate. The systematic variation in the thickness of the gold layer indicated that the interface between the metal layer and the elastomer substrate was diffused and that only part of the metal film contributed to bending stiffness. This effect is associated with the gold clusters' penetration into the silicon. Their findings show the presence of a critical layer thickness that acts as a threshold for the mechanical and electrical properties of the double layer. Only when the threshold is exceeded does percolation of the thin metallic film occur, resulting in linear bending stiffness and electrical conductivity with respect to the thin film thickness. Cramer et al.[77] designed an experimental setup exploiting the scanning kelvin probe microscopy (SKPM) with AFM. Their study demonstrated the feasibility of utilizing SKPM in non-contact mode to detect strain-induced electronic defects on deformed and flexible samples. As a case study, the authors analyzed the strain response of organic thin film transistors, which are composed of TIPS-pentacene and patterned on polymer foils. By bending the transistor substrate, controlled surface strain was induced in the semiconducting layer. Their findings unveiled that the gradual decline in device performance at specific bending radii originated from the emergence of nano-cracks within the microcrystal arrangement of the TIPS-pentacene film. These cracks become discernible due to the abrupt alteration in SKPM surface potential, an outcome of heightened resistance in localized regions. Notably, the microcrystals displayed robust surface adhesion to the flexible dielectric, a characteristic that empowered them to sustain a conductive pathway even post-fracture. This mechanism mitigates the impact of strain on the overall performance.

As in the case of tensile testing, bending testing also allows for investigating the reliability of the device or its components when subjected to a cyclic load, that is, fatigue. Typically, to understand the damaged state of the device, the electrical resistance is monitored during these tests. This makes it possible to study in situ bending-induced electrical properties. For example, Kim et al.[78] examined the bending strains experienced by Cu thin films on flexible polyimide substrates of varying thicknesses. Simultaneously, they tracked the electrical resistance changes in the metal electrode throughout a bending fatigue test. Their findings highlight different fatigue lifetimes of the thin metal electrode, not only depending on its thickness but also depending on the polymeric substrate thickness. A schematic of the setup is shown in Figure 3g.

4. Nanoindentation and Micropillar Compression Test

Nanoindentation stands as an effective technique for investigating material mechanical properties on a small scale, requiring minimal sample preparation. This method is particularly suited for examining thin films or small material volumes situated near the surface. In a typical nanoindentation test, force and displacement are recorded when an indenter is pressed against the surface of the material being measured, with defined loading

**ADVANCED
SCIENCE NEWS**

www.advancedsciencenews.com

**ADVANCED
MATERIALS
TECHNOLOGIES**

www.advmattechnol.de

Table 3. Summary of the discussed in situ nanoindentation and micropillar compression tests. The table shows the properties that can be measured and the kind of sample that can be investigated with the proposed technique as described in the referenced literature.

	Measurements	Samples	References
Nanoindentation	Hardness and elastic modulus	Thin films	Guillonneau et al.[80]
	Viscoelastic response	3D architecture	Lewis et al.[81]
	Phase identification	Bulk	Novotna et al.[82]
Micropillar compression test	Phase identification	Micropillars	Jun et al.[83]

and unloading profiles. Nanoindentation is most often used to measure hardness and elastic modulus, but significant advances have also been made in measuring other mechanical parameters such as hardening exponents, creep parameters, and residual stresses.[79] In **Table 3** is summarized the in situ tests discussed below.

In the context of soft bioelectronic interfaces, this technique allows investigation of how small portions of the sample behave when subjected to compression. It also allows the stiffness in a surface region of the device to be assessed and mapped to estimate any mechanical mismatch with respect to biological tissue. This information is crucial to optimize the material composition to achieve the best performance and biocompatibility. In situ nanoindentation tests are also relevant to investigate the causes that determine the deformation mechanism. In addition, it can provide a method to visualize how the indenter footprint evolves in the sample as the load increases. The contact area is a crucial parameter for being able to evaluate mechanical parameters from the load-displacement curves provided by a nanoindentation test. The data obtained from nanoindentation experiments can be used to validate and refine theoretical models that describe the mechanical behavior of different materials. For example, Guillonneau et al.[80] developed an experimental method to determine the true projected contact area during indentation testing. In particular, the experimental setup was composed of a micro indenter placed inside an SEM. They investigated the pile-up and sink-in effect during the nanoindentation of different thin films such as nanocrystalline nickel, ultrafine-grained aluminum, and fused silica. **Figure 4**a shows the contact area after the nanoindentation experiment. The SEM is used to continuously observe the indentation testing process, allowing for the monitoring of surface deformation modes around the indenter tip. Their findings highlight that the hardness/elastic modulus ratio defines a threshold to what contact mechanics model is appropriate to describe the nanoindentation model. In particular, when the hardness/elastic modulus ratio is small, the pile-up effect will be predominant; while, when the ratio is big the sink-in dominates the deformation of the material under the indenter.

Nanoindentation experiments provide information about how materials respond to mechanical loading, including their elastic and plastic deformation behavior. The combination of nanomechanical testing and direct observation provides insights into the material's behavior, including crack initiation, delamination, stacking, elastic, and plastic deformation, viscoelastic behavior,

and presence of different phases of the material. For example, Lewis et al.[81] designed a method able to microfabricate the sample first and characterize them with the same instrumentation. Exploiting the focused ion beam-induced deposition, they were able to microfabricate platinum-carbon 3D nanoscale structures. The nanomechanical tests were performed using a nanoindentation system inside the same SEM for simultaneous in situ imaging. The real-time imaging during the sample deformation allowed them to record a viscoelastic response of the material under investigation. Figure 4b shows a platinum-carbon 3D architecture before and after the nanoindentation on top. Recently, an AFM-in-SEM setup had been proposed by Novotna et al.[82] Such a setup allowed the exploitation of the imaging capabilities of the two techniques, while an indenter performed the mechanical testing. This hybrid technique combined sample phase identification, precise indentation targeting, and topographical analysis into a single measurement, allowing for comprehensive characterization, as shown in Figure 4c.

Similar to the nanoindentation test is the micropillar compression test. During a micropillar compression test, a rigid indenter is typically placed inside an SEM. To apply this characterization technique, the samples must have a pillar-like structure, which is typically achieved with a focused ion beam. In contrast to nanoindentation, compression testing often employs a flat punch indenter that possesses a slightly larger diameter than the micropillar itself. Consequently, the compression technique is less reliant on the precise indenter geometry. Specimens for compression tests offer a small volume of material with a well-defined shape, typically with cylindrical or square cross-section. The in situ SEM micropillar compression tests provide a means to gauge the uniaxial mechanical response of small material volumes, allowing for direct correlation of stress–strain data with individual deformation occurrences. This approach facilitates the quantification of specific phases and particles, as well as the examination of deformation behavior and strengthening mechanisms. For example, Jun et al.[83] reported a study of local deformation mechanisms in two-phase Ti alloys. Specifically, they conducted micropillar compression tests by employing a displacement-controlled nanoindenter within a SEM, maintaining a constant displacement rate. The outcomes demonstrated a notable influence of the morphology of the two phases on the localized deformation behavior. Snapshots extracted from the time step evolution of the compression test can be seen in Figure 4d.

5. Optimized Soft Bioelectronic Interfaces Via Nanomechanical Characterization

In this section, we describe recent examples from the literature that showcase how in situ nanomechanical characterization methods are relevant to optimize the mechanical properties of soft bioelectronic interfaces. We discuss case studies involving the design of wearable or implantable devices, where in situ nanomechanical testing was used to improve stability, performance, and biocompatibility. These results highlight the potential for future applications in the design of bioelectronic prostheses, implantable sensors, and wearable devices.

The first case study focuses on the design of stretchable low impedance electrodes for recording from small peripheral nerves. In particular, Decataldo et al.[15] showed how in
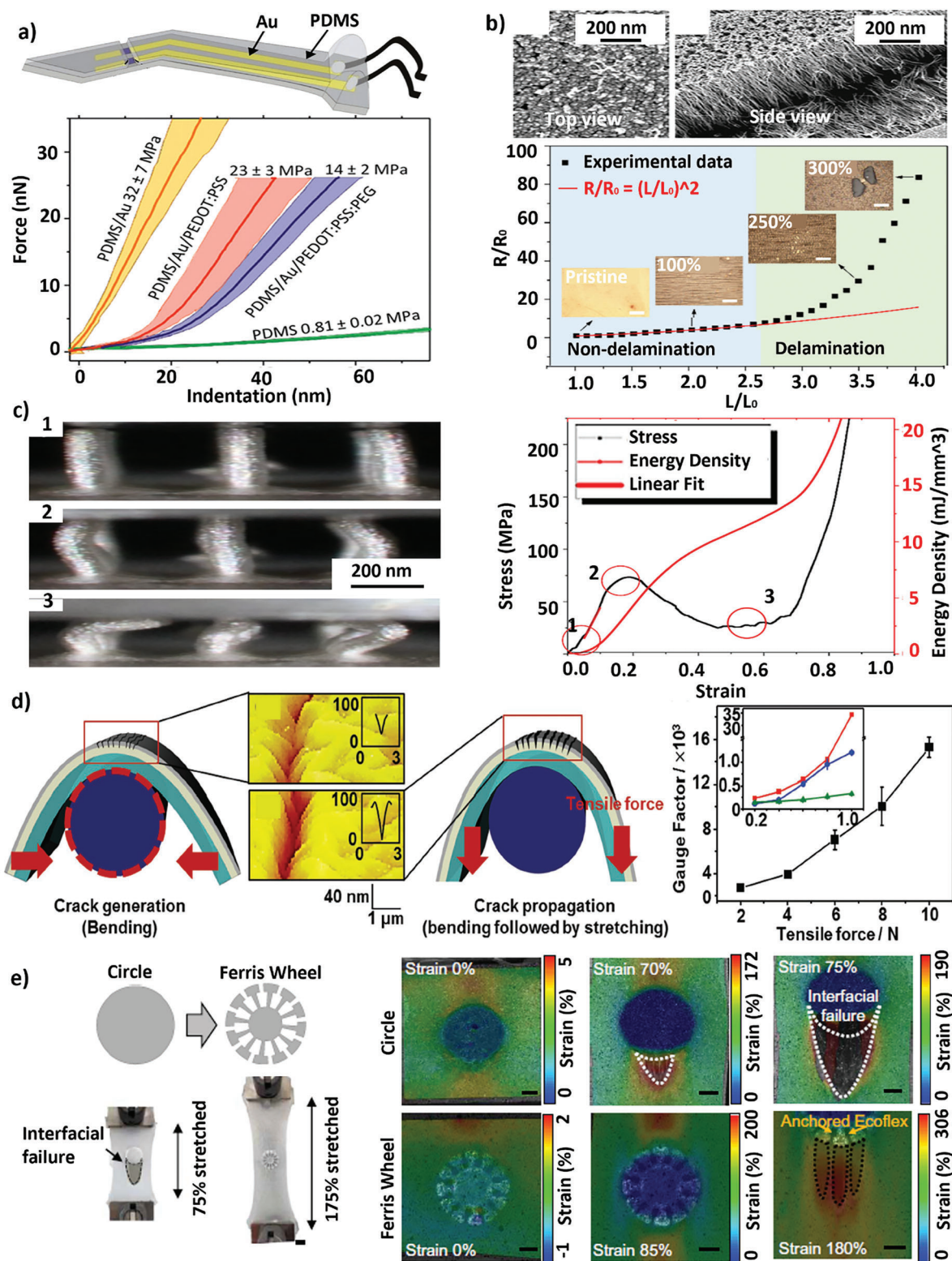
2300931 (9 of 16)
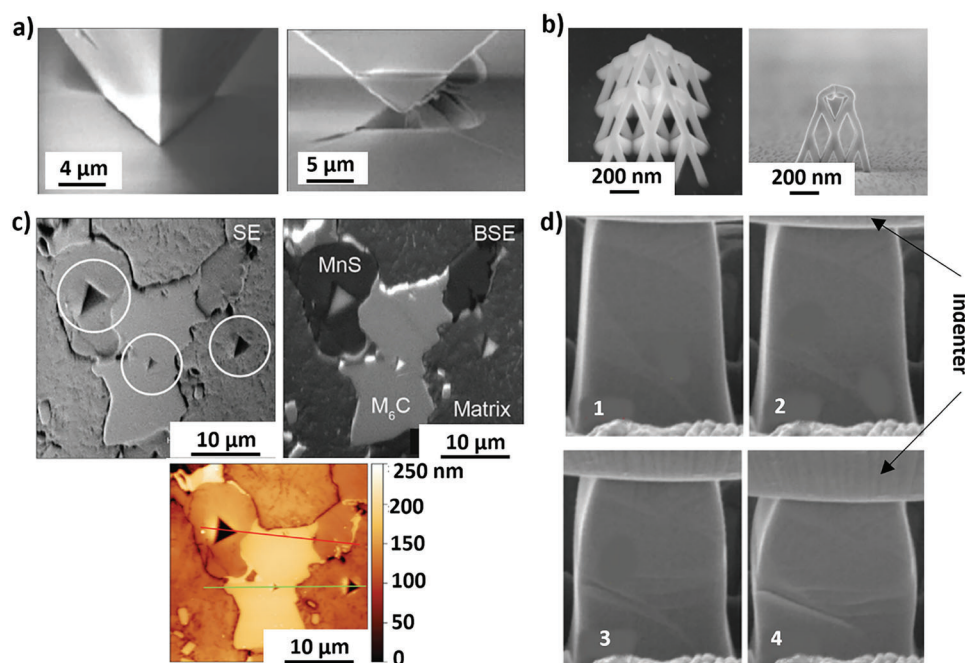
Figure 4. Nanoindentation and Micropillar compression tests. a) The indentation at its peak load and the indentation post-unloading, revealing the material's imprint on the tip that aids in determining the sink-in phenomenon. Reproduced with permission.[80] Copyright 2019, Springer Nature. b) Pyramidal structure before (captured with a 30° tilt) and after (obtained at an 89° angle relative to the electron beam) compression. Reproduced with permission.[81] Copyright 2017, Royal Society of Chemistry. c) SEM image obtained with secondary electrons (SE) with circles highlighting individual indents and SEM image obtained with backscattered electrons (BSE) indicating the material composition. On the bottom, the AFM image of the same region of the sample is shown. The AFM image allows the extraction of the profiles of the nanoindentation imprint into the sample. Reproduced with permission.[82] Copyright 2020, Oxford University Press. d) Time step evolution of the micropillar compression test. Reproduced under the terms of the CC-BY 4.0 license.[83] Copyright 2016, The Authors, published by Elsevier.

situ nanomechanical characterization could be used to optimize the mechanical properties of the stretchable conductive polymer, resulting in improved stability and performance in vivo. Recent advancements in minimally invasive electrodes for recording peripheral sympathetic nerves in small animals had centered on electrode materials featuring both low-impedance ionic/electronic interfaces and elastic mechanical attributes capable of accommodating the soft and delicate nerve fibers. This particular case study introduced a highly stretchable, low-impedance electrode design that employed microcracked gold films as the metallic conductors. These gold films were covered with a stretchable conducting polymer composite to facilitate ion-to-electron exchange. **Figure 5**a illustrates a schematic of the electrode. The conducting polymer composite, consisting of poly(3,4-ethylenedioxythiophene) polystyrene sulfonate (PEDOT:PSS), demonstrated adhesive properties and low impedance, attributes achieved through meticulous control of thickness, plasticizer polyethylene glycol (PEG) content, and deposition conditions. AFM measurements conducted under strain revealed that the optimized conducting polymer coating aligned well with the microcrack mechanics of the underlying gold layer. This allowed the coating to effectively absorb tensile deformation when the electrodes were stretched (as depicted on the right side of Figure 5a). The significance of the PEG plasticizer became evident when examining the electrode properties under tensile strain. By incorporating a plasticizer into the PEDOT:PSS/PEG coating, an electrode was achieved that combined low-impedance characteristics

with elastic stretchability. This electrode maintained impedance levels comparable to unstrained PEDOT:PSS up to a strain of 40%. The efficacy of these stretchable electrodes was validated by successfully recording high-quality renal sympathetic nerve activity in rats under chronic conditions.

The second case study concerned the development of a stretchable conductor based on gold nanowires chemically bonded to an elastomer. Specifically, Wang et al.[84] showed how the electromechanical performance of the material depended on the geometry and position of the nanowires relative to the substrate. Their results show how standing enokitake-like gold nanowires, when chemically bonded to elastomeric materials, can showcase exceptional stretchability, reaching up to 900%. This level of stretchability far surpasses that of conventional vacuum-evaporated bulk metals or percolating nanowire films. A schematic of the enokitake-like sample tested is shown in Figure 5b. To test the electromechanical properties of the samples, they performed an in situ tensile test by studying the relative change in electrical resistance as a function of strain. The morphology of the specimen was monitored during strain using an optical microscope. In order to evaluate the electromechanical response for tensile strain sensing, motorized moving stages were employed to clamp the two ends of the samples. The data acquired for the sample with standing enokitake-like gold nanowires is shown in Figure 5b. Through images acquired with AFM at different strains, they investigated the shape of the microcracks in the different samples. Their discoveries emphasized that exclusively in the

**ADVANCED
SCIENCE NEWS**

www.advancedsciencenews.com

**ADVANCED
MATERIALS
TECHNOLOGIES**

www.advmattechnol.de

Figure 5. Soft bioelectronics interfaces optimized with nanomechanical characterization techniques. a) On the top, scheme showing the stretchable microelectrode for small peripheral nerve recordings. On the bottom, the force-indentation curves acquired with AFM are reported. In the presence of PEDOT:PSS surface coating, the effective modulus of the surface decreases. Adapted under the terms of the CC-BY 4.0 license.[15] Copyright 2019, The Authors, published by Springer Nature. b) On the top, standing enokitake-like gold nanowires chemically bonded to an elastomer. On the bottom, the electromechanical test results are shown along with the optical microscope images acquired during the deformation. Adapted with permission.[84]

**ADVANCED
SCIENCE NEWS**

www.advancedsciencenews.com

**ADVANCED
MATERIALS
TECHNOLOGIES**

www.advmattechnol.de

scenario of vertically aligned nanowires, the cracks' initial shape was V-like, typically occurring at strains below 300%. Subsequently, under more extensive strains, typically ranging between 300% and 800%, the cracks transitioned into large U-shaped patterns that spanned the entire film. In contrast, the remaining samples exhibited the standard U-shaped crack formation from the outset. Ultimately, they established that these stretchable conductors could be harnessed to manufacture inherently stretchable supercapacitors and serve as sensors for facial expression recognition masks, effectively resembling a "second-skin."

The third case study focused on the correlation between fabrication parameters and the mechanical behavior of polycrystalline micropillars 3D printed. Saleh et al.[85] 3D printed several Ag micropillars, varying systematically the grain size. The grain size could be tuned by altering either the initial nanoparticle size or the sintering conditions. They then performed an in situ micropillar compression test using an optical microscope to observe the samples during the deformation (Figure 5c). The grain sizes were determined by identifying boundaries within the SEM images using image processing software. Micropillars with small grain sizes exhibited brittle behavior, and the moment they became unstable, they collapsed. This failure occured without plastic deformation. On the other hand, in the case of coarse grains, buckling occurred at lower stresses than brittle behavior in the previous sample, but the micropillars buckled without breaking. Such fabrication procedure for the micropillars had then been exploited developing an implantable soft device to record brain activity. In particular, the microelectrodes had been designed to enable safe insertion into a mouse brain, avoiding buckling and breakage.[60] To examine the impact of repeated insertions during acute usage on impedance, the researchers introduced microelectrodes tipped with PEDOT:PSS into an agarose phantom brain multiple times. The resulting effect on the electrode impedances was measured. The average impedances consistently remained within the range of 300 to 800 kilohms at a frequency of 1 kHz up to 15 insertions. Notably, no micropillars experienced detachment from the substrate during this process, a fact confirmed through visual inspection after each insertion.

The fourth case study reported the use of in situ bending test to investigate the performances of nanoscale crack-based sensor made of Pt thin film on a polyurethane–acrylates substrate. Park et al.[86] developed an experimental setup that allowed to modulate the crack depth in a two-step process. Initially, the sample was bent around a rod of known radius of curvature to generate the cracks on the metal layer. Then, the crack depth was modulated by applying a tensile force. To monitor the crack depth during bending and stretching, an AFM was used. Their findings highlighted that the sensitivity of the sensor was directly related to the crack depth. Indeed, they found that the deeper the cracks were, the greater the sensitivity was (Figure 5d). Finally, they developed several wearable sensors as proof of enhanced sensitivity. Specifically, sensors positioned across various areas of the hand proved to be effective in discerning motion; while, a sensor situated on the neck facilitated the recognition of voice tones.

The last case study introduced a geometrical solution for integrating rigid islands into a soft polymeric matrix. This strategy involved placing non-stretchable devices on arrays of rigid islands, effectively reducing the lateral strain applied to the devices. This is because the polymer matrix surrounding the islands possessed a lower elastic modulus compared to the islands, leading to predominant stretching of the polymer matrix. However, potential interfacial cracks between the rigid islands and the polymer materials can arise due to mechanical disparities, such as differences in modulus and stretchability. These cracks are likely to occur during excessive or repetitive stretching, eventually resulting in crack propagation and device failure. Yang et al.[87] addressed this issue by presenting geometrically engineered rigid islands that exhibited robust mechanical stability at the interface. They developed an in situ nanomechanical characterization technique to investigate strain distribution and failure modes at the interface between rigid and soft components. Their experimental setup utilized a CCD camera, a strain stage, and a commercially available digital image correlation algorithm program to analyze images captured at various strain levels (Figure 5e). The study considered different island geometries and polymer matrices to optimize the design. The findings of their research underscored the effectiveness of the interlocking structure within the proposed Ferris wheel-shaped island (FWI) design in suppressing crack propagation at the interface. The optimized geometrical shapes of FWIs were dependent on the mechanical properties of the polymer materials used (such as Ecoflex, Dragon Skin, and Ecoflex Gel). This repetitive interlocking structure significantly extended fatigue life against various 3D deformation modes such as twisting, poking, crumpling, and stretching in the 1D direction. Further, the authors demonstrated several practical applications utilizing the FWI array within Ecoflex and an intrinsically stretchable electrode. These applications included stretchable electronics capable of functioning under diverse deformations and electronic skin (e-skin) capable of detecting tactile stimuli.

6. Conclusion

In conclusion, soft bioelectronic interfaces have shown the possibility of monitoring and stimulating physiological processes in vivo. The development of these interfaces has been driven by

---

Copyright 2018, American Chemical Society. c) On the left, micropillar buckling without breaking at different loads during the compression test. The experimental data acquired are reported on the right. Adapted with permission.[85] Copyright 2018, Elsevier. d) On the left, schematics of crack generation via bending and crack propagation to modulate the crack depth via additional stretching. The red arrows indicate the direction of the load applied. The AFM images are acquired during the crack formation and propagation to measure the crack depth. On the right, the dependence of the sensitivity (gauge factor) from the tensile force applied to modulate the crack depth is shown. Reproduced with permission.[86] Copyright 2016, Wiley-VCH GmbH. e) Top left: photographs displaying PLA islands embedded in Ecoflex. Bottom left: Photographs comparing the maximum stretchability of circle-shaped islands (CI) and Ferris wheel-shaped islands (FWI) within an Ecoflex substrate. Notably, the CI achieves a stretch of 75%; while, the FWI reaches a stretch of 175%. Right: Digital Image Correlation (DIC) images offer a visual representation of crack propagation progression for both CI and FWI configurations within Ecoflex during stretching. Reproduced under the terms of the CC-BY 4.0 license.[87] Copyright 2022, The Authors, published by American Association for the Advancement of Science.

---

the need for minimally invasive devices that can provide high-resolution data on biological systems without causing damage or discomfort. With the advent of new materials and fabrication techniques, soft bioelectronics has become increasingly versatile, allowing for the creation of complex devices that can integrate with biological tissues and adapt to their mechanical properties. In this review, we reported experimental techniques for testing mechanical properties in situ at the micro- and nanoscale that are emerging nowadays. Using local in situ nanomechanical characterization techniques, the elastic modulus, adhesion, friction, and other properties of these materials at the nanoscale have been measured, analyzed, and mapped. This information can help guide the design and optimization of soft bioelectronic interfaces and devices, which have numerous applications in areas such as healthcare, robotics, and human–machine interfaces. However, further research is needed to fully understand the complex mechanical behavior of these materials and how it relates to their biological and electronic properties. Despite the progress made, the development and commercialization of soft bioelectronic interfaces still face significant challenges that need to be addressed. These include ensuring biocompatibility to avoid any negative reactions or tissue damage by selecting safe implantation materials and designing interfaces that do not cause inflammation. Achieving the longevity of these interfaces inside the body is also crucial, which requires the development of materials and manufacturing techniques that can withstand the harsh conditions within the body. Moreover, flexibility and stretchability are essential features of soft bioelectronic interfaces to match the shape of biological tissues and organs. However, developing materials that are soft yet mechanically robust remains a major obstacle. Moreover, in situ techniques still show several limitations, such as size constraints of devices impacting accurate measurements and the potential alteration of results due to device manipulation. Delicate preparation is necessary, and handling could introduce artifacts. Maintaining physiological conditions is challenging due to temperature, humidity, and pH variations affecting mechanical behavior. In addition, the majority of the in situ techniques often involve the combined use of two or more instruments; thus, being expensive and difficult to reproduce in other laboratories with other experimental setups. Therefore, future experimental techniques should provide approaches that are easy to access. Despite these limitations, in situ nanomechanical techniques are indispensable for researching bioelectronic interfaces, aiding in device optimization, as highlighted in this review. Looking ahead, the potential future direction for these techniques involves establishing standardized setups that minimize the need for extensive sample manipulation and ensure physiological operating condition during tests, making them applicable to a wide range of different samples. This way, in situ nanomechanical characterization methods could be effectively integrated with other approaches, such as UMT or DMA, enabling a comprehensive understanding of soft bioelectronics devices. Such a methodological advancement in combination with new materials and processing methods will enable a future generation for soft bioelectronic interfaces that integrate seamlessly into the body mechanics while preserving device integrity over long timescales. Only with such low-invasive and durable devices, the prospect of bioelectronic medicine will become a reality leading to novel medical technologies improving human health and quality of life.

Conflict of Interest

The authors declare no conflict of interest.

[1] P. Chen, X. Sun, H. Peng, *Adv. Funct. Mater.* **2020**, *30*, 2001827.

[2] D. Gao, K. Parida, P. S. Lee, *Adv. Funct. Mater.* **2020**, *30*, 1.

[3] T. R. Ray, J. Choi, A. J. Bandodkar, S. Krishnan, P. Gutruf, L. Tian, R. Ghaffari, J. A. Rogers, *Chem. Rev.* **2019**, *119*, 5461.

[4] T. Someya, M. Amagai, *Nat. Biotechnol.* **2019**, *37*, 382.

[5] Y. Liu, M. Pharr, G. A. Salvatore, *ACS Nano* **2017**, *11*, 9614.

[6] G. Yao, C. Yin, Q. Wang, T. Zhang, S. Chen, C. Lu, K. Zhao, W. Xu, T. Pan, M. Gao, Y. Lin, *J. Mater.* **2020**, *6*, 397.

[7] K. W. Cho, S.-H. Sunwoo, Y. J. Hong, J. H. Koo, J. H. Kim, S. Baik, T. Hyeon, D.-H. Kim, *Chem. Rev.* **2022**, *122*, 5068.

[8] X. Chen, K. Parida, J. Wang, J. Xiong, M.-F. Lin, J. Shao, P. S. Lee, *ACS Appl. Mater. Interfaces* **2017**, *9*, 42200.

[9] J.-K. Song, D. Son, J. Kim, Y. J. Yoo, G. J. Lee, L. Wang, M. K. Choi, J. Yang, M. Lee, K. Do, J. H. Koo, N. Lu, J. H. Kim, T. Hyeon, Y. M. Song, D.-H. Kim, *Adv. Funct. Mater.* **2017**, *27*, 1605286.

[10] S.-Z. Guo, K. Qiu, F. Meng, S. H. Park, M. C. Mcalpine, *Adv. Mater.* **2017**, *29*, 1701218.

[11] M.-F. Lin, J. Xiong, J. Wang, K. Parida, P. S. Lee, *Nano Energy* **2018**, *44*, 248.

[12] Y. Liu, J. J. S. Norton, R. Qazi, Z. Zou, K. R. Ammann, H. Liu, L. Yan, P. L. Tran, K.-I. Jang, J. W. Lee, D. Zhang, K. A. Kilian, S. H. Jung, T. Bretl, J. Xiao, M. J. Slepian, Y. Huang, J.-W. Jeong, J. A. Rogers, *Sci. Adv.* **2016**, *2*, e1601185.

[13] C. M. Boutry, A. Nguyen, Q. O. Lawal, A. Chortos, S. Rondeau-Gagné, Z. Bao, *Adv. Mater.* **2015**, *27*, 6954.

[14] J. Viventi, D.-H. Kim, L. Vigeland, E. S. Frechette, J. A. Blanco, Y.-S. Kim, A. E. Avrin, V. R. Tiruvadi, S.-W. Hwang, A. C. Vanleer, D. F. Wulsin, K. Davis, C. E. Gelber, L. Palmer, J. Van Der Spiegel, J. Wu, J. Xiao, Y. Huang, D. Contreras, J. A. Rogers, B. Litt, *Nat. Neurosci.* **2011**, *14*, 1599.

[15] F. Decataldo, T. Cramer, D. Martelli, I. Gualandi, W. S. Korim, S. T. Yao, M. Tessarolo, M. Murgia, E. Scavetta, R. Amici, B. Fraboni, *Sci. Rep.* **2019**, *9*, 10598.

[16] J. Heikenfeld, A. Jajack, J. Rogers, P. Gutruf, L. Tian, T. Pan, R. Li, M. Khine, J. Kim, J. Wang, J. Kim, *Lab Chip* **2018**, *18*, 217.

[17] Y. Dai, Y. Song, J. Xie, G. Xiao, X. Li, Z. Li, F. Gao, Y. Zhang, E. He, S. Xu, Y. Wang, W. Zheng, X. Jiang, Z. Qi, D. Meng, Z. Fan, X. Cai, *ACS Appl. Mater. Interfaces* **2020**, *12*, 41148.

[18] Q. Liang, X. Xia, X. Sun, D. Yu, X. Huang, G. Han, S. M. Mugo, W. Chen, Q. Zhang, *Adv. Sci.* **2022**, *9*, e2201059.

[19] J. S. Heo, J. Eom, Y.-H. Kim, S. K. Park, *Small* **2018**, *14*, 1703034.

[20] S. M. Wellman, J. R. Eles, K. A. Ludwig, J. P. Seymour, N. J. Michelson, W. E. Mcfadden, A. L. Vazquez, T. D. Y. Kozai, *Adv. Funct. Mater.* **2018**, *28*, 1701269.

[21] V. S. Polikov, P. A. Tresco, W. M. Reichert, *J. Neurosci. Methods* **2005**, *148*, 1.

[22] X. Ren, K. Pei, B. Peng, Z. Zhang, Z. Wang, X. Wang, P. K. L. Chan, *Adv. Mater.* **2016**, *28*, 4832.

[23] C. L. Lim, C. Byrne, J. K. Lee, *Ann. Acad. Med. Singap.* **2008**, *37*, 347.

[24] C. Dagdeviren, Y. Shi, P. Joe, R. Ghaffari, G. Balooch, K. Usgaonkar, O. Gur, P. L. Tran, J. R. Crosby, M. Meyer, Y. Su, R. Chad Webb, A. S. Tedesco, M. J. Slepian, Y. Huang, J. A. Rogers, *Nat. Mater.* **2015**, *14*, 728.

[25] C. Wang, X. Li, H. Hu, L. Zhang, Z. Huang, M. Lin, Z. Zhang, Z. Yin, B. Huang, H. Gong, S. Bhaskaran, Y. Gu, M. Makihata, Y. Guo, Y. Lei, Y. Chen, C. Wang, Y. Li, T. Zhang, Z. Chen, A. P. Pisano, L. Zhang, Q. Zhou, S. Xu, *Nat. Biomed. Eng.* **2018**, *2*, 687.

[26] R. Biran, D. C. Martin, P. A. Tresco, *Exp. Neurol.* **2005**, *195*, 115.

[27] H. C. Lee, F. Ejserholm, J. Gaire, S. Currlin, J. Schouenborg, L. Wallman, M. Bengtsson, K. Park, K. J. Otto, *J. Neural Eng.* **2017**, *14*, 036026.

[28] K. Yamashita, H. Sawahata, S. Yamagiwa, S. Yokoyama, R. Numano, K. Koida, T. Kawano, *Lab Chip* **2022**, *22*, 747.

[29] D. A. Kennedy, T. Lee, D. Seely, *Integr. Cancer Ther.* **2009**, *8*, 9.

[30] S. Zhang, H. Zhang, G. Yao, F. Liao, M. Gao, Z. Huang, K. Li, Y. Lin, *J. Alloys Compd.* **2015**, *652*, 48.

[31] J. Ruhhammer, T. Herbstritt, D. Ruh, K. Foerster, C. Heilmann, F. Beyersdorf, F. Goldschmidtboeing, A. Seifert, P. Woias, *Biomed. Microdevices* **2014**, *16*, 815.

[32] D. Khodagholy, J. N. Gelinas, T. Thesen, W. Doyle, O. Devinsky, G. G. Malliaras, G. Buzsáki, *Nat. Neurosci.* **2015**, *18*, 310.

[33] K. Tybrandt, D. Khodagholy, B. Dielacher, F. Stauffer, A. F. Renz, G. Buzsáki, J. Vörös, *Adv. Mater.* **2018**, *30*, 1706520.

[34] Y. Shu, T. Su, Q. Lu, Z. Shang, Q. Xu, X. Hu, *Anal. Chem.* **2021**, *93*, 16222.

[35] S. Kim, J. Malik, J. M. Seo, Y. M. Cho, F. Bien, *Sci. Rep.* **2022**, *12*, 17395.

[36] P. Moshayedi, G. Ng, J. C. F. Kwok, G. S. H. Yeo, C. E. Bryant, J. W. Fawcett, K. Franze, J. Guck, *Biomaterials* **2014**, *35*, 3919.

[37] P.-L. Kang, Y.-H. Lin, K. Settu, C.-S. Yen, C.-Y. Yeh, J.-T. Liu, C.-J. Chen, S.-J. Chang, *Polymers* **2020**, *12*, 1186.

[38] C. Boehler, T. Stieglitz, M. Asplund, *Biomaterials* **2015**, *67*, 346.

[39] E. Borda, L. Ferlauto, J. Schleuniger, A. Mustaccio, F. Lütolf, A. Lücke, S. Fricke, N. Marjanovic, D. Ghezzi, *Adv. Eng. Mater.* **2020**, *22*, 1901403.

[40] D. Kireev, V. Rincón Montes, J. Stevanovic, K. Srikantharajah, A. Offenhäusser, *Front. Neurosci.* **2019**, *13*, 320.

[41] C. Chitrakar, E. Hedrick, L. Adegoke, M. Ecker, *Materials* **2022**, *15*, 1664.

[42] J. H. Koo, J.-K. Song, D.-H. Kim, D. Son, *ACS Mater. Lett.* **2021**, *3*, 1528.

[43] M. Shur, F. Fallegger, E. Pirondini, A. Roux, A. Bichat, Q. Barraud, G. Courtine, S. P. Lacour, *ACS Appl. Bio Mater.* **2020**, *3*, 4388.

[44] Y. H. Cho, Y.-G. Park, S. Kim, J.-U. Park, *Adv. Mater.* **2021**, *33*, 2005805.

[45] T. Zhou, H. Yuk, F. Hu, J. Wu, F. Tian, H. Roh, Z. Shen, G. Gu, J. Xu, B. Lu, X. Zhao, *Nat. Mater.* **2023**, *22*, 895.

[46] X. Wen, B Wang, S. Huang, T. "Leo" Liu, M.-S. Lee, P.-S. Chung, Y. T. Chow, I.-W. Huang, H. G. Monbouquette, N. T. Maidment, P.-Y. Chiou, *Biosens. Bioelectron.* **2019**, *131*, 37.

[47] X. Zhang, A. Zhou, G. Hu, Y. Li, K. Zhang, B. Liu, X. Ning, D. Kong, *Biomater. Sci.* **2021**, *9*, 6950.

[48] K. Il Song, H. Seo, D. Seong, S. Kim, K. J. Yu, Y. C. Kim, J. Kim, S. J. Kwon, H. S. Han, I. Youn, H. Lee, D. Son, *Nat. Commun.* **2020**, *11*, 1.

[49] Y. Liu, J. Li, S. Song, J. Kang, Y. Tsao, S. Chen, V. Mottini, K. Mcconnell, W. Xu, Y.-Q. Zheng, J. B.-H. Tok, P. M. George, Z. Bao, *Nat. Biotechnol.* **2020**, *38*, 1031.

[50] S.-H. Sunwoo, K.-H. Ha, S. Lee, N. Lu, D.-H. Kim, *Annu. Rev. Chem. Biomol. Eng.* **2021**, *12*, 359.

[51] Y. Lin, Y. Fang, J. Yue, B. Tian, *Trends Chem.* **2020**, *2*, 519.

[52] K. D. Harris, A. L. Elias, H.-J. Chung, *J. Mater. Sci.* **2016**, *51*, 2771.

[53] D. Vella, J. Bico, A. Boudaoud, B. Roman, P. M. Reis, *Proc. Natl. Acad. Sci. U. S. A.* **2009**, *106*, 10901.

[54] H. Chen, B.-W. Lu, Y. Lin, X. Feng, *IEEE Electron Device Lett.* **2014**, *35*, 132.

[55] S. P. Lacour, S. Wagner, Z. Huang, Z. Suo, *Appl. Phys. Lett.* **2003**, *82*, 2404.

[56] Y. Leterrier, *Prog. Mater. Sci.* **2003**, *48*, 1.

[57] Y. Leterrier, L. Médico, F. Demarco, J.-A. E. Månson, U. Betz, M. F. Escolà, M. Kharrazi Olsson, F. Atamny, *Thin Solid Films* **2004**, *460*, 156.

[58] Y.-Y. Hsu, M. Gonzalez, F. Bossuyt, F. Axisa, J. Vanfleteren, I. De Wolf, *Thin Solid Films* **2011**, *519*, 2225.

[59] J. C. Barrese, N. Rao, K. Proo, C. Triebwasser, C. Vargas-Irwin, L. Franquemont, J. P. Donoghue, *J. Neural Eng.* **2013**, *10*, 066014.

[60] M. S. Saleh, S. M. Ritchie, M. A. Nicholas, H. L. Gordon, C. Hu, S. Jahan, B. Yuan, R. Bezbaruah, J. W. Reddy, Z. Ahmed, M. Chamanzar, E. A. Yttri, R. P. Panat, *Sci. Adv.* **2022**, *8*, eabj4853.

[61] F. Hang, D. Lu, R. J. Bailey, I. Jimenez-Palomar, U. Stachewicz, B. Cortes-Ballesteros, M. Davies, M. Zech, C. Bödefeld, A. H. Barber, *Nanotechnology* **2011**, *22*, 365708.

[62] Y. Zhu, H. D. Espinosa, *Proc. Natl. Acad. Sci. U. S. A.* **2005**, *102*, 14503.

[63] K. Cao, H. Yang, L. Gao, Y. Han, J. Feng, H. Yang, W. Wang, Y. Lu, *Int. J. Smart Nano Mater.* **2020**, *11*, 265.

[64] M. A. Costa Angeli, F. Caronna, T. Cramer, D. Gastaldi, L. Magagnin, B. Fraboni, P. Vena, *IEEE Sens. J.* **2020**, *20*, 4087.

[65] M. A. C. Angeli, T. Cramer, B. Fraboni, L. Magagnin, D. Gastaldi, P. Vena, *MRS Commun.* **2019**, *9*, 129.

[66] C. Thomas, V. Ferreiro, G. Coulon, R. Seguela, *Polymer* **2007**, *48*, 6041.

[67] G. Cortelli, L. Patruno, T. Cramer, B. Fraboni, S. De Miranda, *ACS Appl. Electron. Mater.* **2022**, *4*, 2831.

[68] E. Cattarinuzzi, R. Lucchini, D. Gastaldi, P. Vena, A. Adami, L. Lorenzelli, *Proc. 2015 18th AISEM Annu. Conf. AISEM 2015* **2015**, 1, https://ieeexplore.ieee.org/document/7066784.

[69] S. M. Kleinendorst, R. Fleerakkers, E. Cattarinuzzi, P. Vena, D. Gastaldi, M. P. F. H. L. Van Maris, J. P. M. Hoefnagels, *Int. J. Solids Struct.* **2020**, *204–205*, 52.

[70] Y.-J. Kim, K. Son, I.-C. Choi, I.-S. Choi, W. Il Park, J. Il Jang, *Adv. Funct. Mater.* **2011**, *21*, 279.

[71] A. Morel, S. Domaschke, V. Urundolil Kumaran, D. Alexeev, A. Sadeghpour, S. N. Ramakrishna, S. J. Ferguson, R. M. Rossi, E. Mazza, A. E. Ehret, G. Fortunato, *Acta Biomater.* **2018**, *81*, 169.

[72] M. Antsov, B. Polyakov, V. Zadin, M. Mets, S. Oras, M. Vahtrus, R. Lõhmus, L. Dorogin, S. Vlassov, *Micron* **2019**, *124*, 102686.

[73] G. Cortelli, L. Grob, L. Patruno, T. Cramer, D. Mayer, B. Fraboni, B. Wolfrum, S. de Miranda, *ACS Appl. Mater. Interfaces* **2023**, *15*, 7602.

[74] L. Angeloni, M. Ganjian, M. Nouri-Goushki, M. J. Mirzaali, C. W. Hagen, A. A. Zadpoor, L. E. Fratila-Apachitei, M. K. Ghatkesar, *Addit. Manuf.* **2021**, *39*, 101858.

[75] J.-O. Abrahamians, B. Sauvet, J. Polesel-Maris, R. Braive, S. Regnier, *IEEE Trans. Rob.* **2014**, *30*, 119.

[76] G. Cortelli, L. Patruno, T. Cramer, M. Murgia, B. Fraboni, S. de Miranda, *ACS Appl. Nano Mater.* **2021**, *4*, 8376.

[77] T. Cramer, L. Travaglini, S. Lai, L. Patruno, S. De Miranda, A. Bonfiglio, P. Cosseddu, B. Fraboni, *Sci. Rep.* **2016**, *6*, 38203.

[78] T.-W. Kim, J.-S. Lee, Y.-C. Kim, Y.-C. Joo, B.-J. Kim, *Materials* **2019**, *12*, 2490.

[79] C. A. Schuh, *Mater. Today* **2006**, *9*, 32.

**ADVANCED
SCIENCE NEWS**

www.advancedsciencenews.com

**ADVANCED
MATERIALS
TECHNOLOGIES**

www.advmattechnol.de

[80] G. Guillonneau, J. M. Wheeler, J. Wehrs, L. Philippe, P. Baral, H. W. Höppel, M. Göken, J. Michler, *J. Mater. Res.* **2019**, *34*, 4086.

[81] B. B. Lewis, B. A. Mound, B. Srijanto, J. D. Fowlkes, G. M. Pharr, P. D. Rack, *Nanoscale* **2017**, *9*, 16349.

[82] V. Novotna, J. Horak, M. Konecny, V. Hegrova, O. Novotny, Z. Novacek, J. Neuman, *Microsc. Today* **2020**, *28*, 38.

[83] T.-S. Jun, G. Sernicola, F. P. E. Dunne, T. B Britton, *Mater. Sci. Eng., A* **2016**, *649*, 39.

[84] Y. Wang, S. Gong, S. J. Wang, X. Yang, Y. Ling, L. W. Yap, D. Dong, G. P. Simon, W. Cheng, W. Cheng, *ACS Nano* **2018**, *12*, 9742.

[85] M. Sadeq Saleh, M. Hamidvishkasougheh, H. Zbib, R. Panat, *Scr. Mater.* **2018**, *149*, 144.

[86] B. Park, J. Kim, D. Kang, C. Jeong, K. S. Kim, J. U. Kim, P. J. Yoo, T. Kim, *Adv. Mater.* **2016**, *28*, 8130.

[87] J. C. Yang, S. Lee, B. S. Ma, J. Kim, M. Song, S. Y. Kim, D. W. Kim, T. S. Kim, S. Park, *Sci. Adv.* **2022**, *8*, eabn3863.

Giorgio Cortelli is a research fellow at the University of Bologna. He received his Ph.D. at the University of Bologna, pursuing his research in collaboration with the Department of Civil, Chemical Environmental, and Material Engineering, and the Department of Physics and Astronomy. His research focuses on experimental methods and predictive models for the nanomechanical characterization of stretchable and flexible conductors, particularly used in the context of soft bioelectronic interfaces.

Tobias Cramer is Associate Professor in Material Physics at the University of Bologna. His research concerns novel semiconductors and multifunctional nanomaterials. He enjoys developing novel atomic force microscopy experiments to provide insight into material properties at the nanoscale. He finds that bioelectronic interfaces offer great research opportunities and will revolutionize medicine in the future.

Luca Patruno is associate professor at the University of Bologna. His interests span from Structure and Solid Mechanics to Fluid Dynamics. His research activity focusses on the use of computational methods for the study and optimization of structures and their dynamic behavior, with particular emphasis on the simulation of wind loads.

**ADVANCED
SCIENCE NEWS**

www.advancedsciencenews.com

**ADVANCED
MATERIALS
TECHNOLOGIES**

www.advmattechnol.de

Beatrice Fraboni is a full professor of Physics at the Faculty of Physics at the University of Bologna. Since 2019, she serves as the Director of the Collegio Superiore of the University of Bologna. Her research activity focuses on the analysis and characterization of the electrical transport properties of organic and inorganic semiconducting materials and of advanced (bio)electronic devices. She coordinates national and international research projects, has published over 150 papers in international refereed journals, and holds ten patents.

Stefano de Miranda received his Ph.D. in Structural Mechanics from the University of Bologna, Italy, in 2001. He is currently full professor of Solid and Structural Mechanics at the Department of Civil, Chemical, Environmental and Materials Engineering of University of Bologna, where he is responsible for the Laboratory of Computational Mechanics. His research interests include numerical modeling and finite element approaches, computational wind engineering, coupled problems, historic masonry structures, and environmental aging of porous materials. He is coordinator of national and international research projects and author of over 100 articles published in international peer-reviewed journals.

2300931 (16 of 16)